

# A New Approach to Control Both Rotation Speed and Axial Rotor Position of Axial Flux Permanent Magnet Motor Base on Sliding Mode Control Combining with PID Control

Duong Quoc Tuan, Nguyen Hong Quang\*

Thai Nguyen University of Technology, Vietnam

\*(Corresponding Author. ORCID: 0000-0002-0433-3094)

## Abstract

The paper proposes a new controller for axial flux permanent magnet (AFPM) motor that adjusts both rotation rotor speed and axial rotor position by combining sliding mode controller and PID controller. The sliding mode control dedicated for speed and axial motion while PID is designed for the current loop. Controlled system performance is validated through a set of simulations.

**Keywords:** AFPM motor, speed controller, axial position controller, sliding mode controller, PID controller.

## I. INTRODUCTION

Axial flux permanent magnet motor (AFPB) finds its important role in electric drive systems [1]. Thanks to the ability of producing torque and force at the same time, AFPM does not require axial bearings that may cause mechanical problems [2]. The axial flux motors are one of the most promising electric drive technologies due to its high-power density. Recent researches target mainly on the design problem of AFPM [3], [4], and [5], very limited number of works looking at control aspect [6]–[10]. Most of the works done on control of AFPM use linear control technique that may result in limited operating range of the motor.

The paper proposes a control technique that combine sliding mode control and PID. The inner loop is designed based on sliding mode control and speed regulator is supported by PID control. The control topology exhibit robust property due to the contribution of sliding mode control.

## II. MODEL OF AXIAL FLUX PERMANENT MAGNET MOTOR

### II.1 Introduction to AFPM motors

In terms of structure, the AFPM motor has its own particular specialists, in details, the stator module may include several types: A single module has one winding set and a dual module has two sets of winding sharing a common core and back-to-back establishment. Similarly, a single rotor module includes only one permanent magnet on one side, and in dual module one, both sides have permanent magnets leaning against each other. In this research, an object with two single module stators

outside and one dual module rotor inside is designated as shown in Fig. 1.

When a three-phase voltage is granted to stator coils, different currents are generated (including current  $i_q$ ) flowing inside, they will interact with the magnetics of rotor to generate torque ( $M$ ) and the currents in phase windings (component  $i_d$ ) of stator generate thrust and drag ( $F$ ) based on the principle of the electromagnet. Thanks to special structure and above-mentioned operating principle, the rotor of the motor will not generate axial displacement although both ends of the shaft have magnetic bearings. It allows the absence of additional axial movement block of the rotor, therefore, the motor structure is being compact. Due to the way of winding roll, the rotational magnetic field generates torques  $M_1$  and  $M_2$  on the same direction on the rotor shaft and generates thrust-drag forces  $F_1$  and  $F_2$  between the rotor and the stator on opposite direction. The total torque ( $M=M_1+M_2$ ) is the summation of the torques but the total force is the difference of the axial attractive forces ( $F=F_1-F_2$ ).

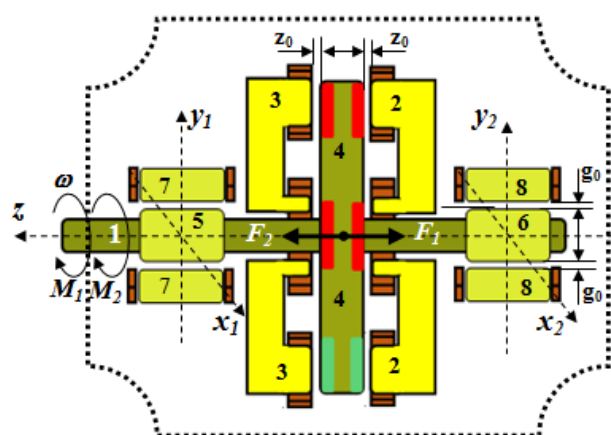


**Fig. 1.** The AFPM motor section with magnetic bearing at both ends integrated (1: The shaft; 2, 3: the stator and the winding of left side and right side of motor; 4: the permanent magnetic rotor of motor; 5, 6: the magnetic bearing rotors on left and right sides; 7, 8: the stator and the winding of magnetic bearing on left and right sides;  $z_0$ ,  $g_0$ : the nominal gaps between the rotor and stator of motor with magnetic bearings)

From the structure and the principle of operation mentioned above, AFPM motor can be considered as two motors that have a common rotor or share a common shaft.

## II.II Mathematical model of AFPM motor

The mathematical model of AFPM motor was developed in  $dq$  coordinate system, as presented as the following. The indicator 1 and 2 are present for the left side motor and right side motor, respectively.

Mathematical model of motor 1:

$$\begin{cases} u_{sd1} = R_s i_{sd1} + L_{sd1} \frac{di_{sd1}}{dt} - \omega_s L_{sq1} i_{sq1} \\ u_{sq1} = R_s i_{sq1} + L_{sq1} \frac{di_{sq1}}{dt} + \omega_s L_{sd1} i_{sd1} + \omega_s \psi_p \end{cases} \quad (1)$$

Mathematical model of motor 2:

$$\begin{cases} u_{sd2} = R_s i_{sd2} + L_{sd2} \frac{di_{sd2}}{dt} - \omega_s L_{sq2} i_{sq2} \\ u_{sq2} = R_s i_{sq2} + L_{sq2} \frac{di_{sq2}}{dt} + \omega_s L_{sd2} i_{sd2} + \omega_s \psi_p \end{cases} \quad (2)$$

Where:

$i_{sd1}, i_{sq1}, i_{sd2}, i_{sq2}$  are the currents on d,q axis of motor 1 and motor 2, respectively,

$u_{sd1}, u_{sq1}, u_{sd2}, u_{sq2}$  are the voltages on d,q axis of motor 1 and motor 2, respectively,

$L_{sd1}, L_{sq1}, L_{sd2}, L_{sq2}$  are the inductances after transformation in dq axis of motor 1 and motor 2, respectively,

$R_s$  is the resistor on stator,

$\psi_p$  is the magnet flux,

$\omega_s$  is the rotation speed of rotor.

The equation that show properties of rotation rotor speed:

$$\frac{3}{2} z_p \left[ \psi_p i_{sq1} + i_{sd1} i_{sq1} (L_{sd1} - L_{sq1}) + \psi_p i_{sq2} + i_{sd2} i_{sq2} (L_{sd2} - L_{sq2}) \right] = m_m + \frac{J}{z_p} \frac{d\omega}{dt} \quad (3)$$

Where:

$m_m$  is the external torque ( the load)

$J$  is the inertia of rotor

$z_p$  is number of dual pole

The equation that show properties of axial rotor position:

$$m \ddot{z} + F_L = k_1 (i_{2d} - i_{1d}) + k_1 (i_{2d} - i_{1d}) z - k_2 z \quad (4)$$

Where:

$z$  is the axial displacement,

$m$  is the mass of rotor,

$F_L$  is the external force influencing on rotor,

$$k_1 = 2 \frac{\mu_0^2 N^2}{g_0^2} \psi_p; \quad k_2 = 2 \frac{\mu_0}{S_p g_0} \psi_p^2.$$

## III. CONTROL DESIGN FOR AFPM MOTOR

In this section, we will design a new algorithm for AFPM motor base on the combination between conventional PID controller and Sliding mode algorithm (SMC). Conventionally, the PID controller applied for this system contains 2 control loop: outer-loop ( speed controller and axial position controller) and inner-loop ( current controller). Using PID for current controller is widely applicable in controlling electric motor, it brings the good performance for system and this algorithm is not too complicate. Especially, when there are some techniques attached like decoupling regulator..., using PID algorithm for current controller loop can achieve the good quality with complicated nonlinear systems as AFPM motor. Meanwhile, the speed and axial position controller loop is more challenging to achieve desired response. Because the responses of this loop will be references for current loop, the performance must be accurate. Beside, during operation, there are some system's parameters that will be changed like load torque, the force influencing rotor...So, conventional PID controller is not good enough to apply in controlling speed and axial position. We propose the sliding mode controller to replace PID. With plenty of outstanding advantages like robust with external disturbances, adjusting with the changes of system's parameters..., the responses of outer-loop will be improve significantly as well as system performance.

### III.I Rotation rotor speed controller

Rewrite the dynamic equation (3) as following:

$$B I_{sq} = m_m + \frac{J}{z_p} \dot{\omega} \quad (5)$$

Where:

$$I_{sq} = \begin{bmatrix} i_{sq1} & i_{sq2} \end{bmatrix}^T$$

$$B = \frac{3}{2} z_p \left[ \psi_p + i_{sd1} (L_{sd1} - L_{sq1}) \quad \psi_p + i_{sd2} (L_{sd2} - L_{sq2}) \right]$$

Choose the sliding surface as:

$$S_\omega = \omega - \omega_r \quad (6)$$

The purpose of control signal is driving the system's state ( in this case is the rotation speed) to the sliding surface, then the controller will drive the sliding surface to zero. So that, there are two components of control signal:

$I_{sqeq}$  is the signal that keep state on the sliding surface, this signal can be computed by condition:  $\dot{S}_\omega = 0$

From (5) and (6), we obtain:

$$\frac{z_p}{J}(BI_{sqeq} - m_m) - \dot{\omega}_r = 0$$

$$\Leftrightarrow I_{sqeq} = B^T (BB^T)^{-1} \left( m_m + \frac{J}{z_p} \dot{\omega}_r \right) \quad (7)$$

$I_{sqsw}$  is the signal that drive the sliding surface to zero, this signal can be computed by condition:  $S_\omega \dot{S}_\omega < 0$

From (5), (6) and above condition, we can choose the control signal as following:

$$I_{sqsw} = B^T (BB^T)^{-1} \frac{J}{z_p} (-c_\omega \text{sign}(S_\omega)) \quad (8)$$

Where  $c_\omega$  is a positive gain

The final control signal is the combination of above signals:

$$I_{sq} = I_{sqeq} + I_{sqsw}$$

$$= B^T (BB^T)^{-1} \left( m_m + \frac{J}{z_p} (\dot{\omega}_r - c_\omega \text{sign}(S_\omega)) \right) \quad (9)$$

We will demonstrate with the controller as (9), the rotation speed will approach the desired value asymptotically through Lyapunov Standard. Let choose the Lyapunov candidate function as:

$$V_\omega = \frac{1}{2} S_\omega^2 \quad (10)$$

The above Lyapunov candidate function have a element that is sliding surface ( or the error value between the response speed and reference). If differential of  $V_\omega$  is negative definite, the element in the Lyapunov candidate function will drive to zero, it means that the rotation speed will be drive to the desired value asymptotically. Take time derivative of (10), we obtain:

$$\dot{V}_\omega = S_\omega \dot{S}_\omega$$

$$= S_\omega \left( \frac{z_p}{J} (BI_{sq} - m_m) - \dot{\omega}_r \right)$$

Replacing the control signal (9) to above equation, we have:

$$\dot{V}_\omega = -c_\omega S_\omega \text{sign}(S_\omega) \leq 0$$

The differential of Lyapunov candidate function is negative definite, the system will be stable as Lyapunov Standard.

### III.II Axial rotor position controller

Rewrite the dynamic equation (4) as:

$$K \Delta I_d - k_2 z - F_L = m \ddot{z} \quad (11)$$

Where:  $K = k_1 + k_1 z$ ;  $\Delta I_d = i_{2d} - i_{1d}$

Choose the sliding surface for axial displacement as:

$$S_z = \lambda z + \dot{z} \quad (12)$$

Where  $\lambda$  is a controller's variable, we will choose  $\lambda$  so that the equation (12) guarantees the Hurwitz Stable Standard. The control signal will drive all components of sliding surface (12) to zero, it means that not only the axial displacement will be drive to zero, but also it's differential will not change. Similarly above section, the control signal in this case also has 2 components, and they can be calculated by these following conditions:

$$\begin{cases} \dot{S}_z = 0 \\ S_z \dot{S}_z < 0 \end{cases} \quad (13)$$

From condition (13), we can compute the signal that keep state (axial displacement) on the sliding surface as:

$$\Delta I_{deq} = \frac{m}{K} (-\lambda \dot{z}) + k_2 z \quad (14)$$

And we choose the signal that drive sliding surface to zero as:

$$\Delta I_{dsw} = \frac{m}{K} (-c_z \text{sign}(S_z)) \quad (15)$$

The final control signal is the combination of the signals (14) and (15):

$$\Delta I_d = \Delta I_{deq} + \Delta I_{dsw}$$

$$= \frac{m}{K} (-\lambda \dot{z} - c_z \text{sign}(S_z)) + k_2 z \quad (16)$$

The steps to demonstrate the stability of the system with above proposed control signal are the same with previous section, choose the Lyapunov candidate function as:

$$V_z = \frac{1}{2} S_z^2$$

After taking time derivative of this Lyapunov candidate function and using the control signal (16), we obtain:

$$\dot{V}_z = -c_z S_z \text{sign}(S_z) \leq 0 \quad (17)$$

The differential of Lyapunov candidate function is negative definite, so the system will be stable with proposed control signal ( or axial displacement will approach zero asymptotically).

### III.III Current controller

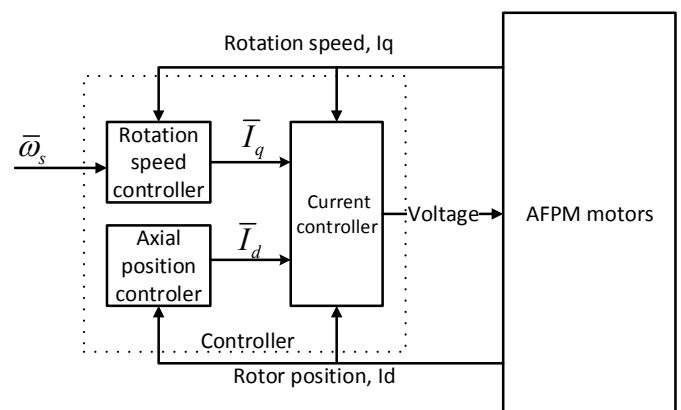


Fig. 2. The structure of the controller

The response of rotation speed controller and axial position controller are the desired value of current controller loop ( as shown in figure 2). We use PID algorithm combining with decoupling regulator to drive stator current to desired values. Input of the controller are the references (from out-loop) and the feedback signals ( currents on dq axis, rotation speed). Output are the voltage signal that will be applied to Stator. Current controller loop are shown in figure 3.

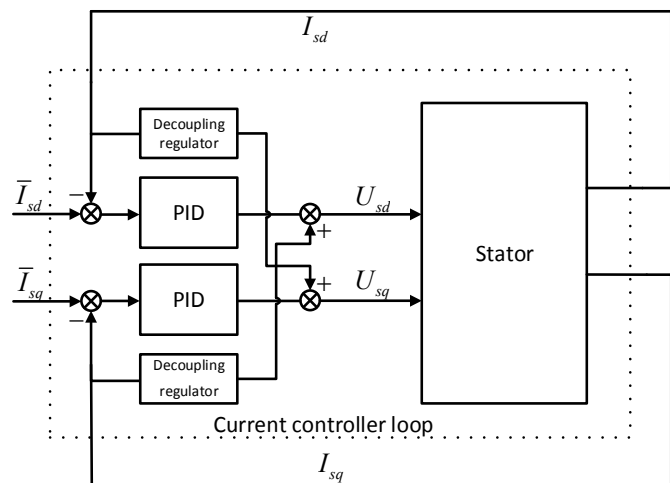


Fig. 3. The structure of the current controller loop

#### IV. SIMULATION RESULTS

Table 1. Parameters of AFPM motor

Parameters	Value
$L_{sd1} = L_{sd2}$	$8,2 \cdot 10^{-6}$ (H)
$L_{sq1} = L_{sq2}$	$9,6 \cdot 10^{-6}$ (H)
$R_s$	2,3 ( $\Omega$ )
$\psi_p$	0,0126 (Wb)
$m$	0,235 (kg)
$J$	0.0000082 ( $\text{kg} \cdot \text{m}^2$ )
$z_p$	1

Case 1: desired rotate speed: 3000 r/m; no load, no external force influencing in rotor.

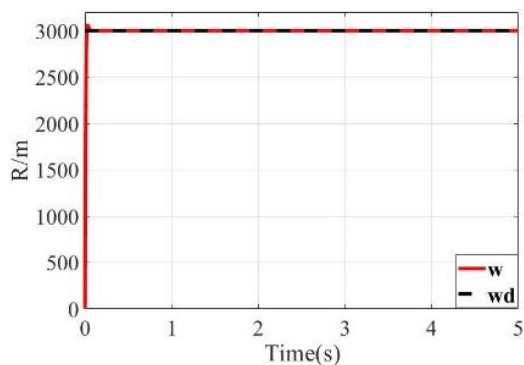


Fig. 4. Rotation speed response case 1

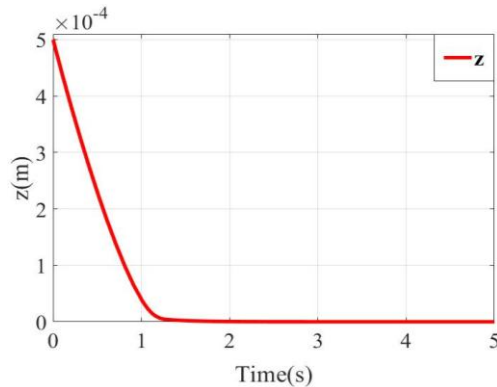


Fig. 5. Axial displacement response case 1

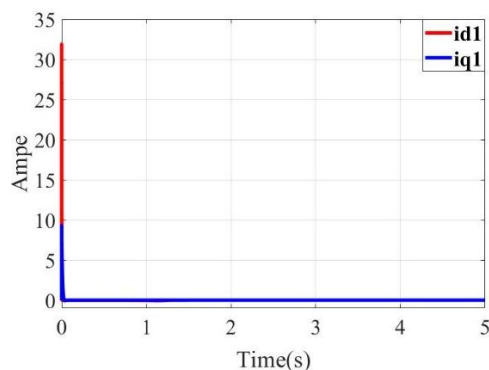


Fig. 6. Current response of Stator 1 case 1

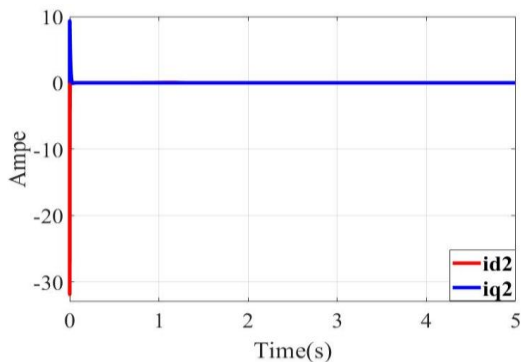


Fig. 7. Current response of Stator 2 case 1

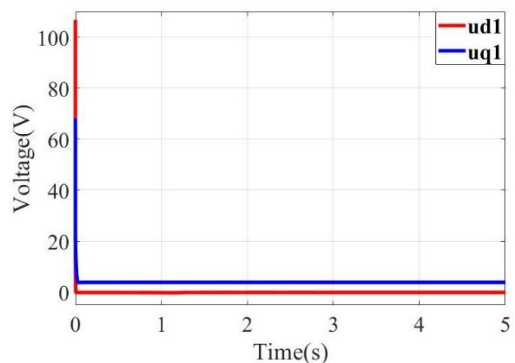
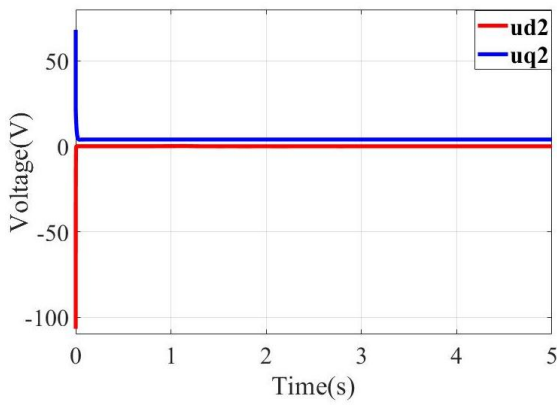


Fig. 8. Control signal of Stator 1 case 1



**Fig. 9.** Control signal of Stator 2 case 1

**Fig. 1** to **Fig 9** show the control performance of the motor in no load condition. It can be seen that the system exhibit good tracking results with applicable input ranges.

**Case 2:** desired rotate speed: 3000 r/m; load = 2 N.m added at 2s; external force influencing in rotor added at 3s.

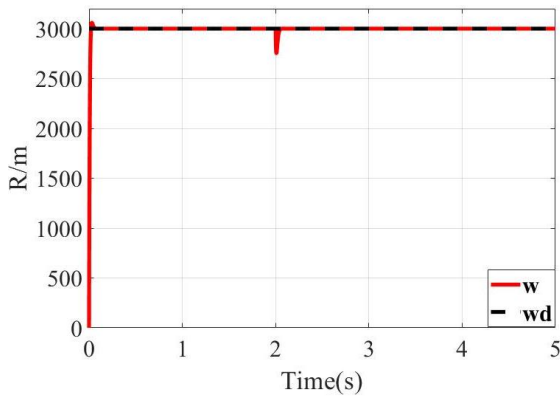


**Fig. 10.** Rotation speed response case 2

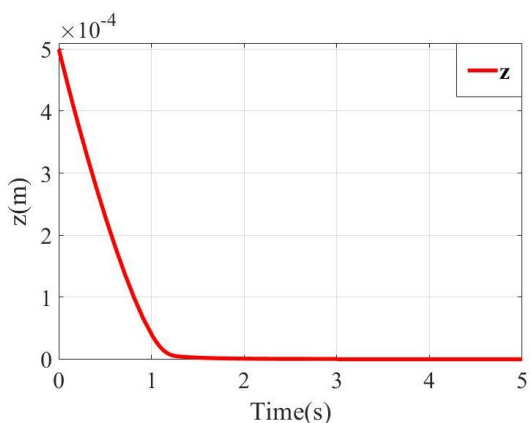


**Fig. 11.** Axial displacement response case 2

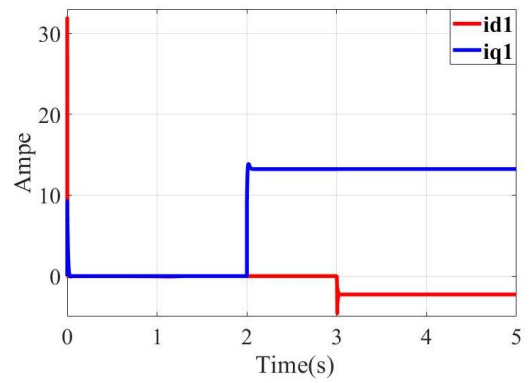


**Fig. 12.** Current response of Stator 1 case 2

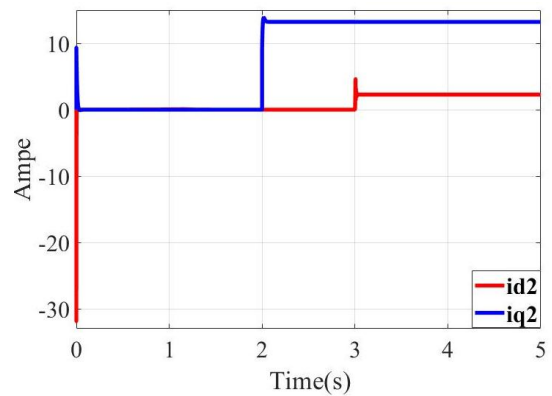


**Fig. 13.** Current response of Stator 2 case 2

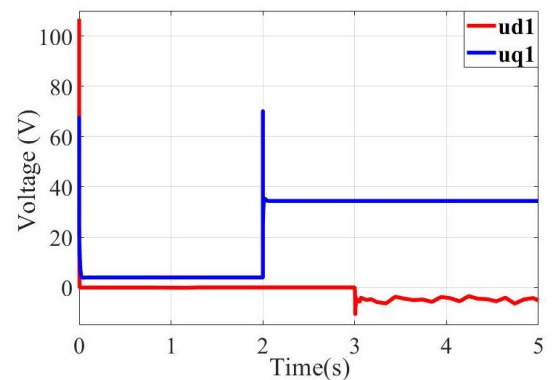


**Fig. 14.** Control signal of Stator 1 case 2

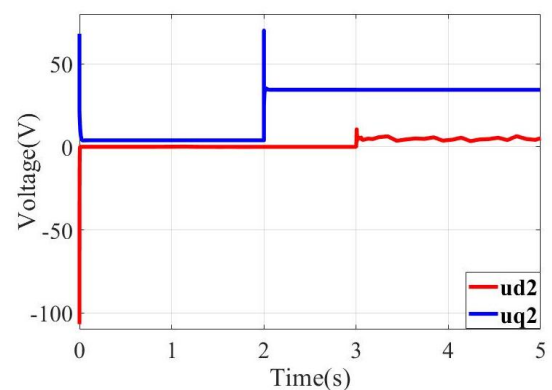


**Fig. 15.** Control signal of Stator 2 case 2

When load and an external force are applied to the system the control still drive the axial position to the equilibrium and the rotational speed to the desired value.

#### IV. CONCLUSION

The paper deal with control problem of an axial flux permanent magnet motor. The control comprised of sliding mode-based control for current loop and PID control for speed loop. The control is verified via numerical simulations.

#### REFERENCES

- [1] L. Bruno, *Axial Flux Permanent Magnet Brushless Machines*, 2nd ed., vol. 53, no. 9. Springer, 2019.
- [2] N. A. Rahim, H. W. Ping, and M. Tadjuddin, "Design of axial flux permanent magnet brushless DC motor for direct drive of electric vehicle," in *2007 IEEE Power Engineering Society General Meeting, 2007*, pp. 1–6.
- [3] Y. P. Yang and J. M. Jiang, "Optimal design of an axial-flux permanent-magnet middle motor integrated in a cycloidal reducer for a pedal electric cycle," *Energies*, vol. 8, no. 12, pp. 14151–14167, 2015.
- [4] S. Zhao, J. Liang, and Y. Zhao, "Optimization design and direct torque control of a flux concentrating axial flux permanent magnet motor for direct driving system," *Electr. Power Components Syst.*, vol. 42, no. 14, pp. 1517–1529, 2014.
- [5] T. I. Mem and K. Fukuda, "A Novel Radial- and Axial-Flux Permanent Magnet Synchronous Motor," vol. 27, no. 1, pp. 1–5, 2019.
- [6] X. M. Tran, N. H. Nguyen, and Q. T. Duong, "Control design for axial flux permanent magnet synchronous motor which operates above the nominal speed," *Adv. Sci. Technol. Eng. Syst.*, vol. 2, no. 3, pp. 153–159, 2017.
- [7] M. H. Shuang Wang, Jianfei Zhao, Tingzhang, "Adaptive Robust Control System for Axial Flux Permanent Magnet Synchronous Motor of Electric," *energies*, vol. 12, 2019.
- [8] F. Jurca and D. Fodorean, "Analysis and control of an axial flux motor for small electric traction system," *IEEE EuroCon 2013*, no. July, pp. 1044–1049, 2013.
- [9] J. Rahmani Fard and M. Ardebili, "Sensor-less control of a novel axial flux-switching permanent-magnet motor," *COMPEL - Int. J. Comput. Math. Electr. Electron. Eng.*, vol. 37, no. 6, pp. 2299–2312, 2018.
- [10] J. Wiśniewski and W. Koczara, "Sensorless control of the axial flux permanent magnet synchronous motor at standstill and at low speed," *CPE 2009 - 6th Int. Conf. - Computability Power Electron.*, no. 7, pp. 463–468, 2009.